East Asian Journal on Applied Mathematics
doi: 10.4208/eajam.240715.050216a

Vol. **6**, No. 2, pp. 152-170
May 2016

An Adaptive Time Stepping Method for Transient Dynamic Response Analysis

Jianguo Huang[1,2,*] and Huashan Sheng[1]

[1] *School of Mathematical Sciences, and MOE-LSC, Shanghai Jiao Tong University, Shanghai 200240, P.R. China.*
[2] *Division of Computational Science, E-Institute of Shanghai Universities, Shanghai 200030, P.R. China.*

Received 24 July 2015; Accepted (in revised version) 5 February 2016.

Abstract. An efficient adaptive time stepping method is proposed for transient dynamic response analysis, which is frequently encountered in civil engineering and elsewhere. The reduced problem following the spatial discretisation can be discretised in the time by a C^0-continuous discontinuous Galerkin method, and the adaptive time stepping strategy is based on optimal *a posteriori* error estimates developed using the energy method. Some numerical experiments demonstrate the effectiveness of our approach.

AMS subject classifications: 65M60, 65M12

Key words: Time stepping method, transient dynamic response, *a posteriori* error analysis, adaptive algorithm.

1. Introduction

It is often important to investigate the time-dependent changes of dynamical systems (their transient response), such as in structure analysis in civil engineering [7]. The underlying mathematical models typically involve a system of second order partial differential equations, which after spatial discretisation by finite element, finite difference or spectral methods reduce to a system of second order ordinary differential equations (ODE) — e.g. see Refs. [3, 12, 14, 19, 20, 27, 30].

The semi-discretised transient dynamic response problem we consider is as follows. For any real $T > 0$, find $\mathbf{u} : [0, T] \to \mathbb{R}^d$ where d is the spatial dimension such that

$$\begin{cases} \mathbf{M}\mathbf{u}'' + \mathbf{C}\mathbf{u}' + \mathbf{K}\mathbf{u} = \mathbf{f}, & 0 < t < T, \\ \mathbf{u}(0) = \mathbf{u}_0, \\ \mathbf{u}'(0) = \mathbf{v}_0. \end{cases} \tag{1.1}$$

*Corresponding author. *Email addresses:* jghuang@sjtu.edu.cn (J. Huang), shs3701001@sjtu.edu.cn (H. Sheng)

 ©2016 Global-Science Press

https://doi.org/10.4208/eajam.240715.050216a Published online by Cambridge University Press

Here the prime denotes differentiation with respect to time; **M**, **C** and **K** are the $d \times d$ global mass, damping and stiffness matrices of the dynamic system, respectively; **u**, $\mathbf{u}'$ and $\mathbf{u}''$ are $d \times 1$ nodal displacement, velocity and acceleration vectors; and **f** is a load function from $[0, T]$ into $\mathbb{R}^d$.

There are many numerical methods for solving the ODE system (1.1). The most widely used include modal superposition [9, 17] and direct-time integration methods such as the Runge-Kutta, central difference, Houbolt, Newmark-β and Wilson-θ procedures — e.g. see Ref. [14] and references therein. Space-time finite element methods provide another widely explored approach for solving second order time-dependent problems [11, 15, 16]. The time-discontinuous Galerkin (TDG) method [11, 18] produces solutions for the displacement and velocity fields together — but it has the disadvantage that an ill-conditioned 4×4 block system must be solved at each time step, which is time consuming. To overcome this drawback, some C^0-continuous time stepping methods were introduced, where the primal variables are involved but only a 2×2 block system has to be solved at each time step [22, 23]. Based on this approach, an adaptive method was proposed for solving second order abstract evolution problems where optimal *a posteriori* error estimates are established [13]. In conjunction with an error equi-distribution strategy and some ideas from the Runge-Kutta-Felberg method, an adaptive time stepping method was produced. In passing, we note that some efficient adaptive time-stepping methods were introduced to simulate the long time dynamics in the molecular beam epitaxy (MBE) model and for the Cahn-Hilliard equations [10, 29, 32, 33].

Here we extend the work in Ref. [13] to develop an adaptive time stepping method for the problem (1.1). Our new contribution is twofold. Although the time discretisation is the same, the derivation of optimal *a posteriori* error estimates is greatly simplified by using the Hermite interpolation polynomial instead of the Legendre polynomial. Our adaptive time stepping method developed from these error estimates is then shown to solve some practical problems very well. The time stepping finite element method for transient dynamic response analysis is discussed in Section 2, and in Section 3 the *a posteriori* error analysis is given in detail. The adaptive algorithm based on the *a posteriori* error estimators is presented in Section 4, followed by its application to the practical problems in Section 5 and our concluding remarks in Section 6.

2. The Time Stepping Finite Element Method

Throughout we assume that **M** and **K** in problem (1.1) are symmetric positive definite matrices, and that **C** is a positive semi-definite matrix. We suppose that

$$\mathbf{u}_0,\ \mathbf{v}_0 \in \mathbb{R}^d, \qquad \mathbf{f} \in L^2(0, T; \mathbb{R}^d). \tag{2.1}$$

We use a standard time stepping method to discretise problem (1.1) — e.g. see [13, 22, 23]. Thus we first partition the time interval $I := (0, T)$ with the nodes

$$0 = t_0 < t_1 < \cdots < t_N = T$$

https://doi.org/10.4208/eajam.240715.050216a Published online by Cambridge University Press

to get the subintervals given by

$$J_n = (t_{n-1}, t_n], \quad k_n = t_n - t_{n-1}, \quad 1 \le n \le N.$$

Define

$$\mathscr{V}_2 = \left\{ \mathbf{v} : \bar{I} \to \mathbb{R}^d;\ \mathbf{v} \in C(\bar{I}),\ \mathbf{v}|_{J_n}(t) = \sum_{j=0}^{2} t^j \mathbf{w}_j,\ \mathbf{w}_j \in \mathbb{R}^d,\ 1 \le n \le N \right\},$$

$$\mathscr{W}_3 = \left\{ \mathbf{v} : \bar{I} \to \mathbb{R}^d; \mathbf{v} \in C^1(\bar{I}),\ \mathbf{v}|_{J_n}(t) = \sum_{j=0}^{3} t^j \mathbf{w}_j,\ \mathbf{w}_j \in \mathbb{R}^d,\ 1 \le n \le N \right\},$$

$$\mathscr{H}_q = \left\{ \mathbf{v} : \bar{I} \to \mathbb{R}^d;\ \mathbf{v}|_{J_n}(t) = \sum_{j=0}^{q} t^j \mathbf{w}_j,\ \mathbf{w}_j \in \mathbb{R}^d,\ 1 \le n \le N \right\}, \quad q = 1, 2, 4.$$

Let $\mathscr{V}_2(J_n)$ and $\mathscr{W}_3(J_n)$ consist of the restrictions to J_n of the element of $\mathscr{V}_2$ and $\mathscr{W}_3$, respectively. Similarly, denote by $\mathscr{H}_q(J_n)$ the restriction of $\mathscr{H}_q$ to J_n. Thus our time stepping method for the problem (1.1) is to find $\mathbf{U} \in \mathscr{V}_2$ such that

$$\begin{cases} \displaystyle\int_{J_n} \left(\left\langle \mathbf{U}'',\ \mathbf{w}' \right\rangle_{\mathbf{M}} + \left\langle \mathbf{U}',\ \mathbf{w}' \right\rangle_{\mathbf{C}} + \left\langle \mathbf{U},\ \mathbf{w}' \right\rangle_{\mathbf{K}} \right) \mathrm{d}t + \left\langle \dot{\mathbf{U}}_+^{n-1} - \dot{\mathbf{U}}_-^{n-1},\ \dot{\mathbf{w}}_+^{n-1} \right\rangle_{\mathbf{M}} \\ \qquad\qquad = \displaystyle\int_{J_n} \left\langle \mathbf{f},\ \mathbf{w}' \right\rangle \mathrm{d}t \quad \forall\, \mathbf{w} \in \mathscr{V}_2(J_n), \quad 1 \le n \le N, \\ \mathbf{U}^0 = \mathbf{u}_0, \quad \dot{\mathbf{U}}_-^0 = \mathbf{v}_0, \end{cases} \tag{2.2}$$

where

$$\begin{aligned} &\langle \mathbf{a}, \mathbf{b} \rangle := \mathbf{b}^{\mathrm{T}} \mathbf{a}, \quad \langle \mathbf{a}, \mathbf{b} \rangle_{\mathbf{A}} := \mathbf{b}^{\mathrm{T}} \mathbf{A} \mathbf{a}, \quad \forall\, \mathbf{a}, \mathbf{b} \in \mathbb{R}^d,\ \mathbf{A} \in \mathbb{R}^{d \times d}, \\ &\dot{\mathbf{w}}_{\pm}^{n-1} := \lim_{s \to 0^+} \mathbf{w}'(t_{n-1} \pm s), \qquad \mathbf{w}^{n-1} := \mathbf{w}(t_{n-1}). \end{aligned} \tag{2.3}$$

Since $\mathbf{U} \in \mathscr{V}_2$, for any $t \in (t_{n-1}, t_n)$ by a direct manipulation we have

$$\begin{cases} \mathbf{U}(t) = \dfrac{1}{k_n^2} \Big((t^2 - 2t_n t + t_n^2) \mathbf{U}^{n-1} + (-t^2 + 2t_n t + t_{n-1}^2 - 2t_n t_{n-1}) \mathbf{U}^n \\ \qquad\qquad + \left(k_n^2 t^2 + (t_{n-1}^2 - t_n^2) t - t_{n-1}^2 t_n + t_{n-1} t_n^2 \right) \dot{\mathbf{U}}_-^n \Big), \\ \mathbf{U}'(t) = \dfrac{1}{k_n^2} \Big((2t - 2t_n) \mathbf{U}^{n-1} + (-2t + 2t_n) \mathbf{U}^n + (2k_n t - t_n^2 + t_{n-1}^2) \dot{\mathbf{U}}_-^n \Big). \end{cases} \tag{2.4}$$

Inserting Eqs. (2.4) into the first equation of (2.2) and taking $\dot{\mathbf{w}}$ to be $\mathbf{w}^*$ or $(t - t_{n-1})\mathbf{w}^*$ where $\mathbf{w}^* \in \mathbb{R}^d$, we find that the method (2.2) is equivalent to finding $\{\mathbf{U}^n\}_{n=0}^N$ and $\{\dot{\mathbf{U}}_-^n\}_{n=0}^N$ such that

$$\begin{aligned} &\begin{bmatrix} \frac{2k_n}{3}\mathbf{K} + \mathbf{C} & -\frac{k_n^2}{6}\mathbf{K} + \mathbf{M} \\ \frac{5k_n^2}{12}\mathbf{K} + \frac{k_n}{3}\mathbf{C} - \mathbf{M} & -\frac{k_n^3}{12}\mathbf{K} + \frac{k_n^2}{6}\mathbf{C} + k_n \mathbf{M} \end{bmatrix} \begin{Bmatrix} \mathbf{U}^n \\ \dot{\mathbf{U}}_-^n \end{Bmatrix} \\ &= \begin{Bmatrix} \mathbf{F}_1 - \frac{k_n}{3}\mathbf{K}\mathbf{U}^{n-1} + \mathbf{C}\mathbf{U}^{n-1} + \mathbf{M}\dot{\mathbf{U}}_-^{n-1} \\ \mathbf{F}_2 - \frac{k_n^2}{12}\mathbf{K}\mathbf{U}^{n-1} + (\frac{k_n}{3}\mathbf{C} - \mathbf{M})\mathbf{U}^{n-1} \end{Bmatrix}, \quad 1 \le n \le N, \end{aligned} \tag{2.5}$$

https://doi.org/10.4208/eajam.240715.050216a Published online by Cambridge University Press

where $\mathbf{F}_1 := \int_{J_n} \mathbf{f} \mathrm{d}t$ and $\mathbf{F}_2 := \int_{J_n} (t - t_{n-1}) \mathbf{f} \mathrm{d}t$.

The above analysis indicates that after the function $\mathbf{U}$ on J_{n-1} is found such that $\mathbf{U}^{n-1}$ and $\dot{\mathbf{U}}_-^{n-1}$ are available, we can obtain $\mathbf{U}^n$ and $\dot{\mathbf{U}}_-^n$ by solving the linear system (2.5) so that the function $\mathbf{U}$ on J_n is obtained. On implementing this computation recursively, we can thereby determine the function $\mathbf{U}$ on the whole time interval $\bar{I}$.

3. *A posteriori* Error Analysis

Define $\mathbf{e} = \mathbf{u} - \mathbf{U}$, with $\mathbf{U}$ given by (2.2). The usual way for bounding the error $\mathbf{e}$ is to use the corresponding error equation

$$\mathbf{M}\mathbf{e}''(t) + \mathbf{C}\mathbf{e}'(t) + \mathbf{K}\mathbf{e}(t) = -\mathbf{M}\mathbf{R}(t)\,,$$

where the residual $\mathbf{R}(t)$ is defined by

$$\mathbf{R}(t) = \mathbf{M}^{-1}\Big(\mathbf{M}\mathbf{U}''(t) + \mathbf{C}\mathbf{U}'(t) + \mathbf{K}\mathbf{U}(t) - \mathbf{f}\Big).$$

However, we can only derive suboptimal *a posteriori* error estimates for the method (2.2), and a crucial step to overcome this drawback is to design a higher order reconstruction $\widetilde{\mathbf{U}}$ or $\widehat{\mathbf{U}}$ from $\mathbf{U}$ [13].

3.1. Reconstruction

As in Ref. [13], we introduce an invertible linear operator $\widetilde{I}_3 : \mathscr{V}_2 \to \mathscr{W}_3$ as follows. With any $\mathbf{w} \in \mathscr{V}_2$ we associate an element $\widetilde{\mathbf{w}} := \widetilde{I}_3 \mathbf{w} \in \mathscr{W}_3$ defined by locally interpolating $\mathbf{w}$ in each subinterval $J_n (1 \le n \le N)$ — i.e. $\widetilde{\mathbf{w}}|_{J_n} \in \mathscr{W}_3(J_n)$ is uniquely determined by

$$\begin{aligned}\widetilde{\mathbf{w}}(t) =& \mathbf{w}^{n-1}\Phi_0\left(\frac{t - t_{n-1}}{k_n}\right) + \mathbf{w}^n\Phi_1\left(\frac{t - t_{n-1}}{k_n}\right) \\ &+ k_n\dot{\mathbf{w}}_-^{n-1}\Psi_0\left(\frac{t - t_{n-1}}{k_n}\right) + k_n\dot{\mathbf{w}}_-^n\Psi_1\left(\frac{t - t_{n-1}}{k_n}\right), \quad 1 \le n \le N\,, \end{aligned} \tag{3.1}$$

where

$$\begin{aligned}&\Phi_0(\xi) = 2\xi^3 - 3\xi^2 + 1\,, \qquad \Psi_0(\xi) = \xi^3 - 2\xi^2 + \xi\,, \\ &\Phi_1(\xi) = -2\xi^3 + 3\xi^2\,, \qquad \Psi_1(\xi) = \xi^3 - \xi^2\,. \end{aligned} \tag{3.2}$$

Here the functions $\Phi_i(\xi)$ and $\Psi_i(\xi)$ $(0 \le i \le 1)$ are the basis functions of Hermite cubic interpolation and we call $\widetilde{\mathbf{w}}$ a time reconstruction of $\mathbf{w}$ — cf. Fig. 1. It is easy to check by the above construction that

$$\int_{J_n} \langle \widetilde{\mathbf{U}}' - \mathbf{U}',\ \mathbf{w}'' \rangle_{\mathbf{M}} \mathrm{d}t = 0 \quad \forall\, \mathbf{w} \in \mathscr{V}_2(J_n)\,,$$

where $\mathbf{U}$ is the solution of (2.2) and $\widetilde{\mathbf{U}}$ is a time reconstruction of $\mathbf{U}$.

https://doi.org/10.4208/eajam.240715.050216a Published online by Cambridge University Press

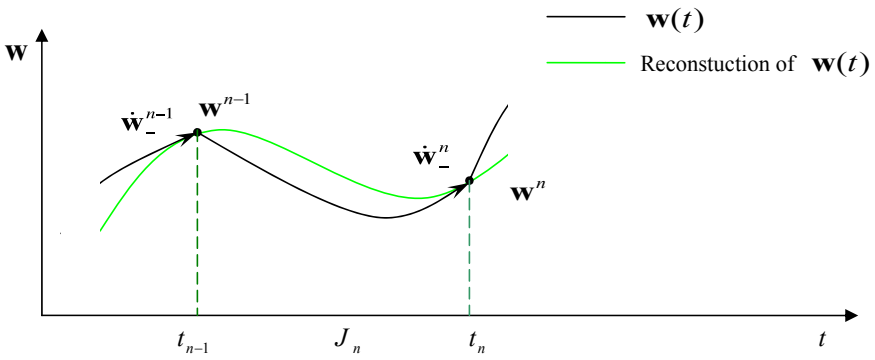


Figure 1: Illustration of $\widetilde{I}_3$.

Consequently, for every $\mathbf{w} \in \mathscr{V}_2(J_n)$, $1 \le n \le N$ we have from integration by parts and the variational equation in (2.2) that

$$\int_{J_n} \left(\langle \widetilde{\mathbf{U}}'', \mathbf{w}' \rangle_{\mathbf{M}} + \langle \mathbf{C}\mathbf{U}' + \mathbf{K}\mathbf{U} - \mathbf{f}, \mathbf{w}' \rangle \right) \mathrm{d}t = 0 \quad \forall\, \mathbf{w} \in \mathscr{V}_2 \quad 1 \le n \le N\,,$$

or equivalently

$$\mathbf{M}\widetilde{\mathbf{U}}'' + P_1(\mathbf{C}\mathbf{U}' + \mathbf{K}\mathbf{U} - \mathbf{f}) = 0 \quad \forall t \in J_n\,, \tag{3.3}$$

where P_q $(q = 1, 2)$ denotes the (local) L^2 orthogonal projection operator onto $\mathscr{H}_q(J_n)$ defined by [2]

$$\int_{J_n} \langle P_q \mathbf{v} - \mathbf{v}, \mathbf{w} \rangle \mathrm{d}t = 0 \quad \forall \mathbf{w} \in \mathscr{H}_q(J_n)\,. \tag{3.4}$$

As shown in Ref. [13], in order to derive the optimal *a posteriori* error estimates an update reconstruction $\widehat{\mathbf{U}}$ from $\mathbf{U}$ is required, and we now proceed as follows.

For $t \in J_n$, $1 \le n \le N$ we define $\widehat{\mathbf{U}} \in \mathscr{H}_4$ by

$$\widehat{\mathbf{U}}(t) = \widetilde{\mathbf{U}}(t) + \mathbf{M}^{-1} \int_{t_{n-1}}^{t} \left(\int_{t_{n-1}}^{\sigma} (P_2 - P_1)(-\mathbf{C}\mathbf{U}'(s) - \mathbf{K}\mathbf{U}(s) + \mathbf{f}(s)) \mathrm{d}s \right) \mathbf{d}\sigma\,. \tag{3.5}$$

Evidently,

$$\widehat{\mathbf{U}}(t_n) = \widetilde{\mathbf{U}}(t_n) = \mathbf{U}(t_n)\,,$$

so $\widehat{\mathbf{U}}$ is continuous on $\bar{I}$. Moreover, on observing that

$$\widehat{\mathbf{U}}'(t) = \widetilde{\mathbf{U}}'(t) + \mathbf{M}^{-1} \int_{t_{n-1}}^{t} (P_2 - P_1)\big(- \mathbf{C}\mathbf{U}'(s) - \mathbf{K}\mathbf{U}(s) + \mathbf{f}(s)\big) \mathrm{d}s$$

for $t \in J_n$, we know that

$$\widehat{\mathbf{U}}'(t_n) = \widetilde{\mathbf{U}}'(t_n) = \dot{\mathbf{U}}_-^n\,,$$

https://doi.org/10.4208/eajam.240715.050216a Published online by Cambridge University Press

hence $\widehat{\mathbf{U}}'(t)$ is also continuous on $\bar{I}$. On the other hand, it is routine to check that

$$\widehat{\mathbf{U}}''(t) = \widetilde{\mathbf{U}}''(t) + \mathbf{M}^{-1}(P_2 - P_1)(-\mathbf{C}\mathbf{U}'(t) - \mathbf{K}\mathbf{U} + \mathbf{f}) , \quad t \in J_n ,$$

which combined with Eq. (3.3) implies

$$\mathbf{M}\widehat{\mathbf{U}}'' + P_2(\mathbf{C}\mathbf{U}' + \mathbf{K}\mathbf{U} - \mathbf{f}) = 0 , \quad t \in J_n . \tag{3.6}$$

3.2. Error estimates

Let $\|\cdot\|$, $\|\cdot\|_{\mathbf{M}}$, $\|\cdot\|_{\mathbf{C}}$ and $\|\cdot\|_{\mathbf{K}}$ denote the norms over $\mathbb{R}^d$ defined by the inner products in (2.3), respectively. We further define

$$\|\mathbf{v}\|_{L^\infty_{\mathbf{M}}(G)} = \operatorname*{ess\,sup}_{t\in G} \|\mathbf{v}(t)\|_{\mathbf{M}} . \tag{3.7}$$

Under the assumption (2.1), we know that there exists a unique weak solution

$$\mathbf{u} \in C\left([0,T];\ \mathbb{R}^d\right) \cap C^1\left([0,T];\ \mathbb{R}^d\right)$$

to the transient dynamic problem (1.1).

Let $\widetilde{\mathbf{e}} := \mathbf{u} - \widetilde{\mathbf{U}}$ and $\widehat{\mathbf{e}} := \mathbf{u} - \widehat{\mathbf{U}}$. Let $\widetilde{\mathbf{R}}$ and $\widehat{\mathbf{R}}$ be the residuals of $\widetilde{\mathbf{U}}$ and $\widehat{\mathbf{U}}$, respectively — i.e. we have

$$\widetilde{\mathbf{R}}(t) := \mathbf{M}^{-1}\left(\mathbf{M}\widetilde{\mathbf{U}}''(t) + \mathbf{C}\widetilde{\mathbf{U}}'(t) + \mathbf{K}\widetilde{\mathbf{U}}(t) - \mathbf{f}(t)\right) , \ t \in J_n , 1 \le n \le N , \tag{3.8}$$

$$\widehat{\mathbf{R}}(t) := \mathbf{M}^{-1}\left(\mathbf{M}\widehat{\mathbf{U}}''(t) + \mathbf{C}\widehat{\mathbf{U}}'(t) + \mathbf{K}\widehat{\mathbf{U}}(t) - \mathbf{f}(t)\right) , \ t \in J_n , 1 \le n \le N . \tag{3.9}$$

Then respectively subtracting Eqs. (3.8) and (3.9) from the equation in (1.1), we obtain

$$\mathbf{M}\widetilde{\mathbf{e}}''(t) + \mathbf{C}\widetilde{\mathbf{e}}'(t) + \mathbf{K}\widetilde{\mathbf{e}}(t) = -\mathbf{M}\widetilde{\mathbf{R}}(t) , \tag{3.10}$$

$$\mathbf{M}\widehat{\mathbf{e}}''(t) + \mathbf{C}\widehat{\mathbf{e}}'(t) + \mathbf{K}\widehat{\mathbf{e}}(t) = -\mathbf{M}\widehat{\mathbf{R}}(t) . \tag{3.11}$$

Now we test Eq. (3.10) by $\widetilde{\mathbf{e}}'$ to get on integration over $t \in [0,\ \tau]$:

$$\int_0^\tau \left(\langle\widetilde{\mathbf{e}}''(s),\ \widetilde{\mathbf{e}}'(s)\rangle_{\mathbf{M}} + \langle\widetilde{\mathbf{e}}'(s),\ \widetilde{\mathbf{e}}'(s)\rangle_{\mathbf{C}} + \langle\widetilde{\mathbf{e}}(s),\ \widetilde{\mathbf{e}}'(s)\rangle_{\mathbf{K}}\right)\mathrm{d}s = \int_0^\tau \langle -\widetilde{\mathbf{R}}(s),\ \widetilde{\mathbf{e}}'(s)\rangle_{\mathbf{M}}\ \mathrm{d}s , \tag{3.12}$$

whence after integration by parts and noting that $\widetilde{\mathbf{e}}(0) = \widetilde{\mathbf{e}}'(0) = 0$ we have

$$\frac{1}{2}\|\widetilde{\mathbf{e}}'(\tau)\|^2_{\mathbf{M}} + \int_0^\tau \|\widetilde{\mathbf{e}}'(s)\|^2_{\mathbf{C}}\ \mathrm{d}s + \frac{1}{2}\|\widetilde{\mathbf{e}}(\tau)\|^2_{\mathbf{K}} = \int_0^\tau \langle -\widetilde{\mathbf{R}}(s)\ ,\ \widetilde{\mathbf{e}}'(s)\rangle_{\mathbf{M}}\ \mathrm{d}s\ ,\ \tau \in [0,t] . \tag{3.13}$$

From Eq. (3.13) and the Cauchy-Schwarz inequality we immediately have

$$\begin{aligned}\frac{1}{2}\left(\max_{0\le\tau\le t}\|\widetilde{\mathbf{e}}'(\tau)\|_{\mathbf{M}}\right)^2 &\le \max_{0\le\tau\le t}\int_0^\tau |\langle\widetilde{\mathbf{R}}(s),\ \widetilde{\mathbf{e}}'(s)\rangle_{\mathbf{M}}|\ \mathrm{d}s \\ &\le \int_0^t |\langle\widetilde{\mathbf{R}}(s),\ \widetilde{\mathbf{e}}'(s)\rangle_{\mathbf{M}}|\ \mathrm{d}s\ \le\ \max_{0\le\tau\le t}\|\widetilde{\mathbf{e}}'(\tau)\|_{\mathbf{M}}\int_0^t \|\widetilde{\mathbf{R}}(s)\|_{\mathbf{M}}\ \mathrm{d}s ,\end{aligned}$$

https://doi.org/10.4208/eajam.240715.050216a Published online by Cambridge University Press

implying that

$$\max_{0\le\tau\le t}\|\widetilde{\mathbf{e}}'(\tau)\|_{\mathbf{M}}\le 2\int_0^t\|\widetilde{\mathbf{R}}(s)\|_{\mathbf{M}}\,\mathrm{d}s\,. \tag{3.14}$$

A similar argument from Eq. (3.11) produces a similar estimate for $\widehat{\mathbf{e}}(t)$. In summary, we obtain the following theorem.

Theorem 3.1. *Let* $\mathbf{u}$ *and* $\mathbf{U}$ *denote the solution of the problem* (1.1) *and the method* (2.2), *respectively. Let* $\widetilde{\mathbf{U}}$ *be the reconstruction of* $\mathbf{U}$ *by* (3.1) *and* $\widehat{\mathbf{U}}$ *the reconstruction of* $\mathbf{U}$ *by* (3.5). *Then for any* $t\in[0,T]$,

$$\max_{0\le\tau\le t}\|(\mathbf{u}-\widetilde{\mathbf{U}})'(\tau)\|_{\mathbf{M}}\le 2\int_0^t\|\widetilde{\mathbf{R}}(s)\|_{\mathbf{M}}\,\mathrm{d}s\,, \tag{3.15}$$

$$\max_{0\le\tau\le t}\|(\mathbf{u}-\widehat{\mathbf{U}})'(\tau)\|_{\mathbf{M}}\le\ 2\int_0^t\|\widehat{\mathbf{R}}(s)\|_{\mathbf{M}}\,\mathrm{d}s\,, \tag{3.16}$$

where $\widetilde{\mathbf{R}}$ *and* $\widehat{\mathbf{R}}$ *are given by Eqs.* (3.8) *and* (3.9), *respectively.*

We next discuss the efficiency of the above *a posteriori* error estimates.

Lemma 3.1. *For* $t\in J_n$ *and* $1\le n\le N$,

$$\mathbf{U}(t)-\widetilde{\mathbf{U}}(t)=-\frac{1}{6}k_n^3\widetilde{\mathbf{U}}^{(3)}\Psi_0\left(\frac{t-t_{n-1}}{k_n}\right), \tag{3.17}$$

$$\widehat{\mathbf{U}}(t)-\widetilde{\mathbf{U}}(t)=\frac{1}{24}k_n^4\widehat{\mathbf{U}}^{(4)}\Lambda\left(\frac{t-t_{n-1}}{k_n}\right), \tag{3.18}$$

where Ψ_0 *is defined in* (3.2) *and* $\Lambda(\xi)=\xi^2(1-\xi)^2$. *Moreover, for* $1\le n\le N$

$$\left\|(\mathbf{U}-\widetilde{\mathbf{U}})'\right\|_{L^\infty_{\mathbf{M}}(J_n)}=\frac{1}{6}k_n^2\|\widetilde{\mathbf{U}}^{(3)}\|_{L^\infty_{\mathbf{M}}(J_n)}\,, \tag{3.19}$$

$$\left\|(\widehat{\mathbf{U}}-\widetilde{\mathbf{U}})'\right\|_{L^\infty_{\mathbf{M}}(J_n)}=\frac{\sqrt{3}}{216}k_n^3\|\widehat{\mathbf{U}}^{(4)}\|_{L^\infty_{\mathbf{M}}(J_n)}\,,\quad 1\le n\le N\,. \tag{3.20}$$

Furthermore, we have

$$\begin{aligned}2\int_0^t\|\widetilde{\mathbf{R}}(s)\|_{\mathbf{M}}\,\mathrm{d}s\le\sum_{m-1}^{n}\Bigg(&\frac{1}{3}k_m^3\|\mathbf{C}\widetilde{\mathbf{U}}^{(3)}\|_{L^\infty_{\mathbf{M}^{-1}}(J_m)}+\frac{1}{36}k_m^4\|\mathbf{K}\widetilde{\mathbf{U}}^{(3)}\|_{L^\infty_{\mathbf{M}^{-1}}(J_m)}\\&+\frac{\sqrt{3}}{27}k_m^3\|\mathbf{K}\mathbf{U}''\|_{L^\infty_{\mathbf{M}^{-1}}(J_m)}+2\int_{J_m}\|\mathbf{f}(s)-P_1\mathbf{f}(s)\|_{\mathbf{M}^{-1}}\,\mathrm{d}s\Bigg),\end{aligned} \tag{3.21}$$

$$\begin{aligned}2\int_0^t\|\widehat{\mathbf{R}}(s)\|_{\mathbf{M}}\,\mathrm{d}s\le\sum_{m-1}^{n}\Bigg(&\frac{\sqrt{3}}{216}k_n^4\|\mathbf{C}\widehat{\mathbf{U}}^{(4)}\|_{L^\infty_{\mathbf{M}^{-1}}(J_m)}+\frac{1}{3}k_m^3\|\mathbf{C}\widetilde{\mathbf{U}}^{(3)}\|_{L^\infty_{\mathbf{M}^{-1}}(J_m)}\\&+\frac{1}{360}k_m^5\|\mathbf{K}\widehat{\mathbf{U}}^{(4)}\|_{L^\infty_{\mathbf{M}^{-1}}(J_m)}+\frac{1}{36}k_m^4\|\mathbf{K}\widetilde{\mathbf{U}}^{(3)}\|_{L^\infty_{\mathbf{M}^{-1}}(J_m)}\\&+2\int_{J_m}\|\mathbf{f}(s)-P_2\mathbf{f}(s)\|_{\mathbf{M}^{-1}}\,\mathrm{d}s\Bigg).\end{aligned} \tag{3.22}$$

https://doi.org/10.4208/eajam.240715.050216a Published online by Cambridge University Press

Proof. Instead of an expansion in terms of Legendre polynomials as in Refs. [13, 21], the Hermite interpolation formula is used below and simplifies the mathematical argument significantly. From the definitions of $\mathbf{U}$ and $\widetilde{\mathbf{U}}$, for $t \in J_n$ we have $1 \le n \le N$,

$$\widetilde{\mathbf{U}}(t) = \mathbf{U}^{n-1}\Phi_0(\xi) + \mathbf{U}^n\Phi_1(\xi) + k_n\dot{\mathbf{U}}_-^{n-1}\Psi_0(\xi) + k_n\dot{\mathbf{U}}_-^n\Psi_1(\xi)\,, \tag{3.23}$$

$$\mathbf{U}(t) = \mathbf{U}^{n-1}\Phi_0(\xi) + \mathbf{U}^n\Phi_1(\xi) + k_n\dot{\mathbf{U}}_+^{n-1}\Psi_0(\xi) + k_n\dot{\mathbf{U}}_-^n\Psi_1(\xi)\,, \tag{3.24}$$

where $\xi = (t - t_{n-1})/k_n$. From some direct computation, it follows that

$$\mathbf{U}(t) - \widetilde{\mathbf{U}}(t) = k_n(\dot{\mathbf{U}}_+^{n-1} - \dot{\mathbf{U}}_-^{n-1})\Psi_0(\xi)\,, \tag{3.25}$$

$$\widetilde{\mathbf{U}}^{(3)}(t) = -\frac{6}{k_n^2}(\dot{\mathbf{U}}_+^{n-1} - \dot{\mathbf{U}}_-^{n-1})\,, \quad t \in J_n\,, \tag{3.26}$$

where Ψ_0 is defined in (3.2) and $\dot{\mathbf{U}}_+^{n-1} = 2(\mathbf{U}^n - \mathbf{U}^{n-1})/k_n - \dot{\mathbf{U}}_-^n$. On the other hand, differentiating Eq. (3.25) with respect to t gives

$$(\mathbf{U} - \widetilde{\mathbf{U}})'(t) = (\dot{\mathbf{U}}_+^{n-1} - \dot{\mathbf{U}}_-^{n-1})\Psi_0'\left(\frac{t - t_{n-1}}{k_n}\right), \quad t \in J_n\,,$$

which yields

$$\|(\mathbf{U} - \widetilde{\mathbf{U}})'\|_{L^\infty_{\mathbf{M}}(J_n)} = \|\dot{\mathbf{U}}_+^{n-1} - \dot{\mathbf{U}}_-^{n-1}\|_{\mathbf{M}}\,, \quad 1 \le n \le N\,,$$

hence we obtain Eqs. (3.17) and (3.19). Next, recalling $\widehat{\mathbf{U}}$ in Eq. (3.5) and observing that the function values and derivatives of $\widehat{\mathbf{U}}(t) - \widetilde{\mathbf{U}}(t)$ vanish at the endpoints of each J_n, on each J_n $(1 \le n \le N)$ by direct computation we have

$$\widehat{\mathbf{U}}(t) - \widetilde{\mathbf{U}}(t) = 24\widehat{\mathbf{U}}^{(4)}(t - t_{n-1})^2(t_n - t)^2$$

and thus we readily obtain (3.18) and (3.20). In view of these results, we can derive the estimates (3.21) and (3.22) by using the same argument as in Ref. [13]. □

Remark 3.1. It follows from Eq. (3.6) that

$$\widehat{\mathbf{U}}^{(4)} = \mathbf{M}^{-1}\left(P_2(\mathbf{f} - \mathbf{C}\mathbf{U}' - \mathbf{K}\mathbf{U})\right)'' = \mathbf{M}^{-1}\left(-\mathbf{K}\mathbf{U}'' + (P_2\mathbf{f})''\right)\,, \tag{3.27}$$

so we can readily compute the constant vector $\widehat{\mathbf{U}}^{(4)}$.

Let us now proceed to discuss the lower and upper *a posteriori* error bounds for the method (2.2). From the triangle inequality and inequalities (3.15) and (3.19) we obtain

$$\|(\mathbf{u} - \mathbf{U})'\|_{L^\infty_{\mathbf{M}}(0,t)} \le \frac{1}{6}\max_{1\le m\le n} k_m^2\|\widetilde{\mathbf{U}}^{(3)}\|_{L^\infty_{\mathbf{M}}(J_m)} + 2\int_0^t \|\widetilde{\mathbf{R}}(s)\|_{\mathbf{M}}\,\mathrm{d}s\,. \tag{3.28}$$

Again, from the triangle inequality

$$\|(\mathbf{u} - \widetilde{\mathbf{U}})'\|_{L^\infty_{\mathbf{M}}(0,t)} \le \max_{0\le\tau\le t}\|(\mathbf{u} - \widehat{\mathbf{U}})'(\tau)\|_{\mathbf{M}} + \|(\widehat{\mathbf{U}} - \widetilde{\mathbf{U}})'(\tau)\|_{L^\infty_{\mathbf{M}}(0,t)}\,,$$

https://doi.org/10.4208/eajam.240715.050216a Published online by Cambridge University Press

so in conjunction with inequality (3.16) and Eq. (3.20) we have

$$\max_{0\le\tau\le t}\|(\mathbf{u}-\widetilde{\mathbf{U}})'(\tau)\|_{\mathbf{M}} \le \frac{\sqrt{3}}{216}\max_{1\le m\le n} k_m^3\|\widehat{\mathbf{U}}^{(4)}\|_{L_{\mathbf{M}}^{\infty}(J_m)} + 2\int_0^t \|\widehat{\mathbf{R}}(s)\|_{\mathbf{M}}\,\mathrm{d}s\,. \tag{3.29}$$

Thus from Eq. (3.19), the estimates (3.28) and (3.29) and the triangle inequality we obtain

$$\|(\mathbf{U}-\widetilde{\mathbf{U}})'\|_{L_{\mathbf{M}}^{\infty}(0,t)} \le \max_{0\le\tau\le t}\|(\mathbf{u}-\widetilde{\mathbf{U}})'(\tau)\|_{\mathbf{M}} + \|(\mathbf{u}-\mathbf{U})'(\tau)\|_{L_{\mathbf{M}}^{\infty}(0,t)}\,,$$

and hence the following result.

Theorem 3.2 (lower and upper bounds)**.** *Let* $\mathbf{u}$ *and* $\mathbf{U}$ *be the solution of the problem* (1.1) *and the method* (2.2)*, respectively. Then if* $\widetilde{\mathbf{U}}$ *is the reconstruction of* $\mathbf{U}$ *by* (3.1) *and* $\widehat{\mathbf{U}}$ *the reconstruction of* $\mathbf{U}$ *by* (3.5)*, for* $t\in[0,T]$*,* $1\le n\le N$ *we have*

$$\begin{aligned}\frac{1}{6}\max_{1\le m\le n} k_m^2\|\widetilde{\mathbf{U}}^{(3)}\|_{L_{\mathbf{M}}^{\infty}(J_m)} &\le \|(\mathbf{u}-\mathbf{U})'\|_{L_{\mathbf{M}}^{\infty}(0,t)} + \max_{0\le\tau\le t}\|(\mathbf{u}-\widetilde{\mathbf{U}})'(\tau)\|_{\mathbf{M}}\\ &\le \frac{1}{6}\max_{1\le m\le n} k_m^2\|\widetilde{\mathbf{U}}^{(3)}\|_{L_{\mathbf{M}}^{\infty}(J_m)} + 2\int_0^t \|\widetilde{\mathbf{R}}(s)\|_{\mathbf{M}}\,\mathrm{d}s\\ &\quad + \frac{\sqrt{3}}{216}\max_{1\le m\le n} k_m^3\|\widehat{\mathbf{U}}^{(4)}\|_{L_{\mathbf{M}}^{\infty}(J_m)} + 2\int_0^t \|\widehat{\mathbf{R}}(s)\|_{\mathbf{M}}\,\mathrm{d}s\,,\end{aligned} \tag{3.30}$$

where the a posteriori quantities $\widetilde{\mathbf{R}}$ *and* $\widehat{\mathbf{R}}$ *are given by* (3.8) *and* (3.9)*, respectively.*

4. Adaptive Algorithm

Based on the *a posteriori* error estimates given in Theorem 3.2, we can now construct an adaptive time stepping method related to the time stepping method (2.2) as follows.

Let ϵ be the total error tolerance allowed for the *a posteriori* error estimate in (3.30) — i.e.

$$\begin{aligned}\eta :=& \frac{1}{6}\max_{1\le n\le N} k_n^2\|\widetilde{\mathbf{U}}^{(3)}\|_{L_{\mathbf{M}}^{\infty}(J_n)} + \frac{\sqrt{3}}{216}\max_{1\le n\le N} k_n^3\|\widehat{\mathbf{U}}^{(4)}\|_{L_{\mathbf{M}}^{\infty}(J_n)}\\ &+ 2\int_0^T \left(\|\widetilde{\mathbf{R}}(s)\|_{\mathbf{M}} + \|\widehat{\mathbf{R}}(s)\|_{\mathbf{M}}\right)\mathrm{d}s \;\le\; \epsilon\,.\end{aligned} \tag{4.1}$$

To ensure inequality (4.1) holds, we can adjust the time step size k_n such that the following conditions are satisfied:

$$\begin{aligned}\Theta_1 &:= \frac{1}{6}\,k_n^2\|\widetilde{\mathbf{U}}^{(3)}\|_{L_{\mathbf{M}}^{\infty}(J_n)} \;\le\; \frac{1}{3}\epsilon\,,\\ \Theta_2 &:= \frac{\sqrt{3}}{216}\,k_n^3\|\widehat{\mathbf{U}}^{(4)}\|_{L_{\mathbf{M}}^{\infty}(J_n)} \;\le\; \frac{1}{3}\epsilon\,,\\ \Theta_3 &:= 2\frac{T}{k_n}\int_{J_n}\left(\|\widetilde{\mathbf{R}}(s)\|_{\mathbf{M}} + \|\widehat{\mathbf{R}}(s)\|_{\mathbf{M}}\right)\mathrm{d}s \;\le\; \frac{1}{3}\epsilon\,.\end{aligned}$$

https://doi.org/10.4208/eajam.240715.050216a Published online by Cambridge University Press

Then we can use the time-stepping strategy

$$\Theta := 3\ \max\{\ \Theta_1,\ \ \Theta_2,\ \ \Theta_3\ \}\ \ \leq\ \epsilon\,. \tag{4.2}$$

Next, let us consider how to compute the quantities Θ_1, Θ_2 and Θ_3 after we get $\mathbf{U}(t)$ at each time step. First of all, from Eq. (3.26) and the definition of Θ_1 we have

$$\Theta_1 = \left\| \frac{2}{k_n}(\mathbf{U}^n - \mathbf{U}^{n-1}) - \dot{\mathbf{U}}_-^n - \dot{\mathbf{U}}_-^{n-1} \right\|_{\mathbf{M}}\,, \tag{4.3}$$

and secondly from some direct manipulation

$$\Theta_2 = \frac{\sqrt{3}}{216} k_n^3 \left\| \mathbf{M}^{-1}((P_2\mathbf{f})'' - \mathbf{K}\mathbf{U}'') \right\|_{\mathbf{M}}\,, \tag{4.4}$$

and we can compute each term appearing in (4.4) as follows. From the definition of P_2 (cf. (3.4)) and some direct computation,

$$(P_2\mathbf{f})'' = 2\left(\frac{180}{k_n^5}\mathbf{F}_3 - \frac{180}{k_n^4}\mathbf{F}_2 + \frac{30}{k_n^3}\mathbf{F}_1 \right), \tag{4.5}$$

where $\mathbf{F}_i := \int_{J_n} (t - t_{n-1})^{i-1}\mathbf{f}\,\mathrm{d}t$ for $i = 1,2,3$. From (2.4),

$$\mathbf{U}'' = \frac{2}{k_n^2}\left(k_n\dot{\mathbf{U}}_-^n - \mathbf{U}^n + \mathbf{U}^{n-1} \right), \tag{4.6}$$

hence Θ_2 can be obtained using Eqs. (4.4)-(4.6).

To derive Θ_3 we obtain $\widetilde{\mathbf{R}}(t)$ and $\widehat{\mathbf{R}}(t)$ in advance, so from (3.23)

$$\begin{aligned}
\widetilde{\mathbf{U}}(t) &= \mathbf{U}^{n-1}\Phi_0(\xi) + \mathbf{U}^n\Phi_1(\xi) + k_n\dot{\mathbf{U}}_-^{n-1}\Psi_0(\xi) + k_n\dot{\mathbf{U}}_-^n\Psi_1(\xi)\,,\\
\widetilde{\mathbf{U}}'(t) &= \frac{1}{k_n}\left(\mathbf{U}^{n-1}\Phi_0'(\xi) + \mathbf{U}^n\Phi_1'(\xi) + k_n\dot{\mathbf{U}}_-^{n-1}\Psi_0'(\xi) + k_n\dot{\mathbf{U}}_-^n\Psi_1'(\xi) \right),\\
\widetilde{\mathbf{U}}''(t) &= \frac{1}{k_n^2}\left(\mathbf{U}^{n-1}\Phi_0''(\xi) + \mathbf{U}^n\Phi_1''(\xi) + k_n\dot{\mathbf{U}}_-^{n-1}\Psi_0''(\xi) + k_n\dot{\mathbf{U}}_-^n\Psi_1''(\xi) \right),
\end{aligned}$$

where $\xi = (t - t_{n-1})/k_n$, and Φ_0, Φ_1 and Ψ_0, Ψ_1 are the basis functions of the Hermite cubic interpolation — cf. (3.2). Similarly, it follows from Eqs. (3.18), (3.27), (4.5) and (4.6) that

$$\begin{aligned}
\widehat{\mathbf{U}}(t) &= \widetilde{\mathbf{U}}(t) + \frac{1}{24}k_n^4\,\widehat{\mathbf{U}}^{(4)}\Lambda(\xi)\,,\\
\widehat{\mathbf{U}}'(t) &= \widetilde{\mathbf{U}}'(t) + \frac{1}{24}k_n^3\,\widehat{\mathbf{U}}^{(4)}\Lambda'(\xi)\,,\\
\widehat{\mathbf{U}}''(t) &= \widetilde{\mathbf{U}}''(t) + \frac{1}{24}k_n^2\,\widehat{\mathbf{U}}^{(4)}\Lambda''(\xi)\,,
\end{aligned}$$

where $\xi = (t - t_{n-1})/k_n$ and $\Lambda(\xi) = \xi^2(1-\xi)^2$. Then substituting $\widetilde{\mathbf{U}}(t)$ and $\widehat{\mathbf{U}}(t)$ into (3.8) and (3.9) respectively, we obtain $\widetilde{\mathbf{R}}(t)$ and $\widehat{\mathbf{R}}(t)$.

https://doi.org/10.4208/eajam.240715.050216a Published online by Cambridge University Press

In actual computation, the required integration to obtain Θ_3 can be carried out using the Gaussian quadrature formula [31]. Thus for $t \in J_n$ and $1 \le n \le N$ we have

$$\int_{J_n} \left(\|\widetilde{\mathbf{R}}(t)\|_{\mathbf{M}} + \|\widehat{\mathbf{R}}(t)\|_{\mathbf{M}} \right) \mathrm{d}t \doteq \sum_{j=1}^{N_g} \left(\|\widetilde{\mathbf{R}}(t_{n-1} + k_n \zeta_j)\|_{\mathbf{M}} + \|\widehat{\mathbf{R}}(t_{n-1} + k_n \zeta_j)\|_{\mathbf{M}} \right) \omega_j k_n , \quad (4.7)$$

where ζ_j and ω_j $(1 \le j \le N_g)$ are the respective Gaussian quadrature points and weights on the reference interval $[0,1]$.

Given the above preparation, similar to Ref. [13], we introduce algorithms below to compute the numerical solution for the problem (1.1) via the adaptive time stepping strategy. In deriving the time stepping rule, we use the well known error equi-distribution strategy [6,26] and some ideas implicit in the Runge-Kutta-Felberg method [31].

Algorithm 4.1 Computation at each time step.

Input: t_{n-1}, k_n, $\mathbf{U}^{n-1}$, $\dot{\mathbf{U}}_-^{n-1}$
Output: $\mathbf{U}^n$, $\dot{\mathbf{U}}_-^n$, Θ
- **Step 1**: Compute the vector value of $\mathbf{F}_1$, $\mathbf{F}_2$, $\mathbf{F}_3$ in (4.5)
- **Step 2**: Get the numerical solution $\mathbf{U}^n$, $\dot{\mathbf{U}}_-^n$ by (2.5)
- **Step 3:** Get the first term of strategy Θ_1 by (4.3)
- **Step 4:** Get the second term of strategy Θ_2 by (4.5), (4.6) and (4.4)
- **Step 5:** Get $\widetilde{\mathbf{R}}(t)$, $\widehat{\mathbf{R}}(t)$ at Gaussian points by (4.7), (3.8) and (3.9)
- **Step 6:** Summation to get the value of Θ_3 by (4.7)
- **Step 7:** Output $\mathbf{U}^n$, $\dot{\mathbf{U}}_-^n$, and Θ by (4.2)

Algorithm 4.2 Time step size control.

Given a error tolerance ϵ, a parameter $\delta \in (0,1)$, and the max (min) time step size $k_{\max}$ ($k_{\min}$) by user
- **Step 0:** Initialise $n = 1$, $t_0 = 0$, $k_1 = k_{\max}$, $\mathbf{U}^0 = \mathbf{u}_0$, $\dot{\mathbf{U}}_-^0 = \mathbf{v}_0$
- **WHILE** $t_{n-1} < T$
- **Step 1:** Get $\mathbf{U}^n$, $\dot{\mathbf{U}}_-^n$, Θ by Algorithm 4.1 with t_{n-1}, k_n, $\mathbf{U}^{n-1}$, $\dot{\mathbf{U}}_-^{n-1}$
- **Step 2:** If $\delta\epsilon \le \Theta \le \epsilon$, $k_{n+1} = k_n$, go to Step 5
- **Step 3:** If $\Theta < \delta\epsilon$, $k_{n+1} = \min\{2k_n,\ k_{\max}\}$, go to Step 5
- **Step 4:** If $\Theta > \epsilon$, $k_n = \max\{k_n/2,\ k_{\min}\}$, go to Step 1
- **Step 5:** Let $t_n = t_{n-1} + k_n$, $n = n+1$, go to loop condition judgment
- **END WHILE**

5. Numerical Experiments

Throughout this section, we adopt the international system (SI) but omit mentioning the units when there can be no confusion. Moreover, to focus our investigation we only

https://doi.org/10.4208/eajam.240715.050216a Published online by Cambridge University Press

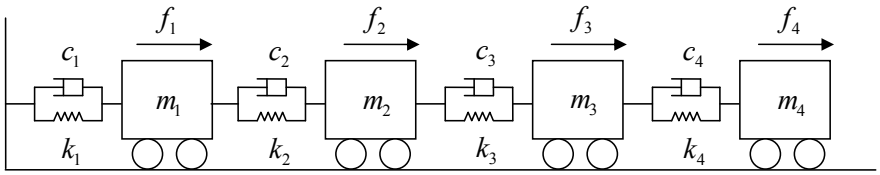


Figure 2: Example 5.1. Lumped mass system.

Table 1: Example 5.1. Mass, damping and stiffness matrices.

M				**K**				**C**			
1e3	0	0	0	30e3	-15e3	0	0	70	-30	0	0
0	1e3	0	0	-15e3	30e3	-15e3	0	-30	70	-30	0
0	0	1e3	0	0	-15e3	30e3	-15e3	0	-30	70	-30
0	0	0	1e3	0	0	-15e3	15e3	0	0	-30	40

consider transient dynamic response analysis for Rayleigh damping systems, such that in the problem (1.1) we have $\mathbf{C} = \alpha\mathbf{M} + \beta\mathbf{K}$, where the constants α and β are the Rayleigh damping coefficients [5,8,25].

5.1. Efficiency of the estimators

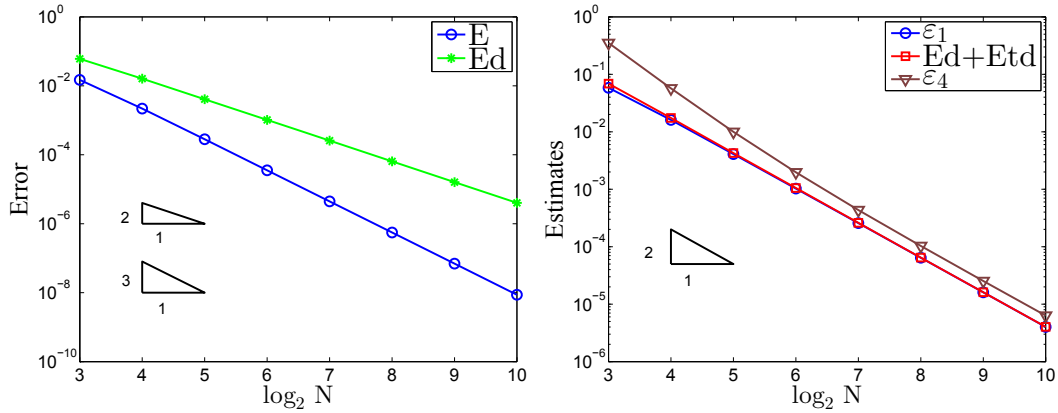
Example 5.1 (Lumped mass system)**.** To illustrate the effectiveness of the *a posteriori* error estimates developed in this contribution, we first study a multi-structure model used by Vikas & Arora [4]. As shown in Fig. 2, the structure consists of four rigid elements (vehicles) with lumped masses m_1, m_2, m_3 and m_4 inter-connected by springs with damping. In our computation, we chose equal masses $m_1 = m_2 = m_3 = m_4 = 1000$ kg and equal spring stiffnesses $k_1 = k_2 = k_3 = k_4 = 15$ kN/m. The assumed values of the structural Rayleigh damping coefficients were $\alpha = 10^{-2}$ and $\beta = 2 \times 10^{-3}$.

From the data the mass, damping and stiffness matrices ($\mathbf{M}$, $\mathbf{C}$ and $\mathbf{K}$) are as shown in Table 1. We chose $T = 2$, noted the exact solution $\mathbf{u}(t) = 0.1\sin(t)(1,-1,1,-1)^T$ so the force term $\mathbf{f}$ can be computed from (1.1), and solved the system using the the method (2.2) in our simulation.

For a given natural number N, we adopted a uniform partition in time with mesh size $k_n = T/N$, $1 \le n \le N$. To show the computational performance of our method, we defined

$$\begin{aligned}
\mathrm{E} &= \max_{0\le\tau\le 2} \|(\mathbf{u}-\mathbf{U})(\tau)\|_{\mathbf{K}}\,,\\
\mathrm{Ed} &= \max_{0\le\tau\le 2} \|(\mathbf{u}-\mathbf{U})'(\tau)\|_{\mathbf{M}}\,,\\
\mathrm{Etd} &= \max_{0\le\tau\le 2} \|(\mathbf{u}-\widetilde{\mathbf{U}})'(\tau)\|_{\mathbf{M}}\,,
\end{aligned}$$

https://doi.org/10.4208/eajam.240715.050216a Published online by Cambridge University Press



(a) Order of E and Ed (b) Order of ε_1 and ε_4

Figure 3: Example 5.1. Numerical results corresponding to estimators in Theorem 3.2.

$$\varepsilon_1 = \frac{1}{6}\max_{1\le n\le N} k_n^2 \|\widetilde{\mathbf{U}}^{(3)}\|_{L^\infty_{\mathbf{M}}(J_n)} ,$$
$$\varepsilon_2 = \frac{\sqrt{3}}{216}\max_{1\le n\le N} k_n^3 \|\widehat{\mathbf{U}}^{(4)}\|_{L^\infty_{\mathbf{M}}(J_n)} ,$$
$$\varepsilon_3 = 2\int_0^2 \|\widetilde{\mathbf{R}}(s)\|_{\mathbf{M}}\, \mathrm{d}s + 2\int_0^2 \|\widehat{\mathbf{R}}(s)\|_{\mathbf{M}}\, \mathrm{d}s ,$$
$$\varepsilon_4 = \eta = \varepsilon_1 + \varepsilon_2 + \varepsilon_3 .$$

In Fig. 3(a) we present the values of E and Ed, as well as their orders 3 and 2, respectively. The numerical results agree with the theoretical estimates in Ref. [23]. In Fig. 3(b) we give the values of *a posteriori* estimators ε_1 and ε_4, as well as their orders. These numerical results demonstrate the theoretical results in Theorem 3.2.

Next, we studied the efficiency of the lower and upper estimators in Theorem 3.2, using the indices given in Ref. [1]. With respect to the reference error Ed + Etd, we defined the lower and upper effectivity indices by

$$\mathrm{Effld} = \frac{\varepsilon_1}{\mathrm{Ed}+\mathrm{Etd}}, \qquad \mathrm{Effud} = \frac{\varepsilon_4}{\mathrm{Ed}+\mathrm{Etd}}.$$

We present the values of these effectivity indices in Fig. 4, from which we can observe that $0.99 \approx \mathrm{Effld} < 1 < \mathrm{Effud} \approx 1.57$ so the *a posteriori* error estimates given in Theorem 3.2 are seen to be rather efficient.

5.2. Efficiency of the adaptive algorithm

Example 5.2 (Lumped mass system)**.** In order to test the effectiveness of our adaptive Algorithm 4.2, we reconsidered the previous model again, but assumed $T = 1$ and the right term $\mathbf{f}$ to be such that the exact solution of the problem (1.1) is

$$\mathbf{u} = 10^{-2}\left(1-\exp(-10000(t-1/2)^2)\right)(1,-1,1,-1)^T .$$

https://doi.org/10.4208/eajam.240715.050216a Published online by Cambridge University Press

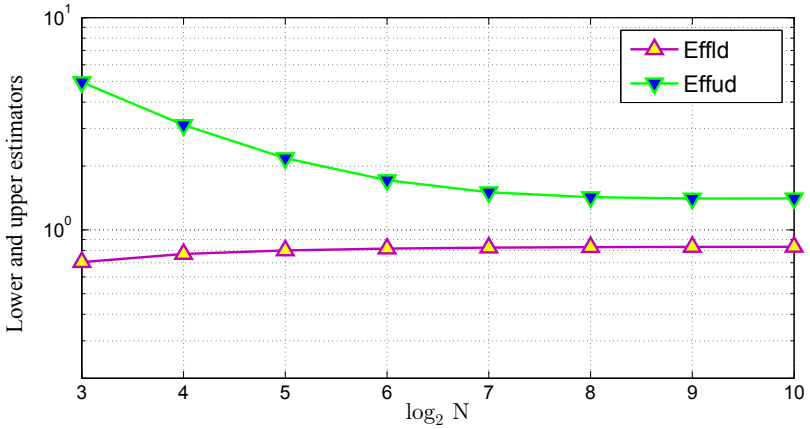
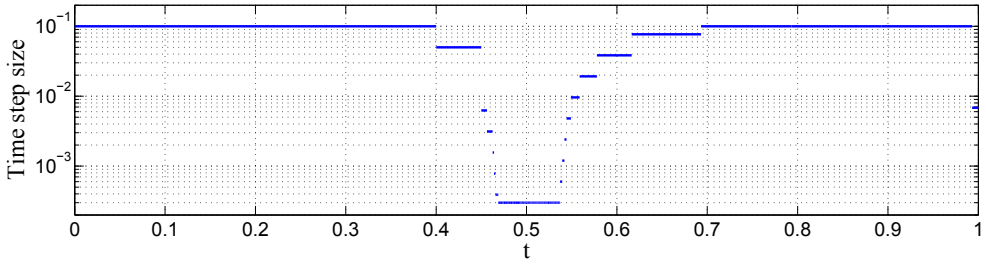
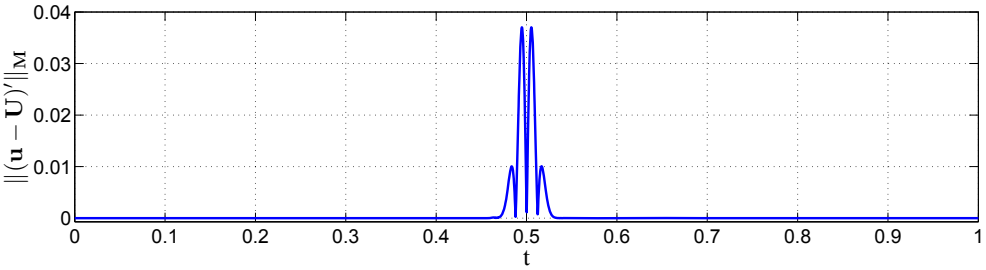


Figure 4: Example 5.1. Effectivity of the indices of lower and upper estimators.



(a) Time step size

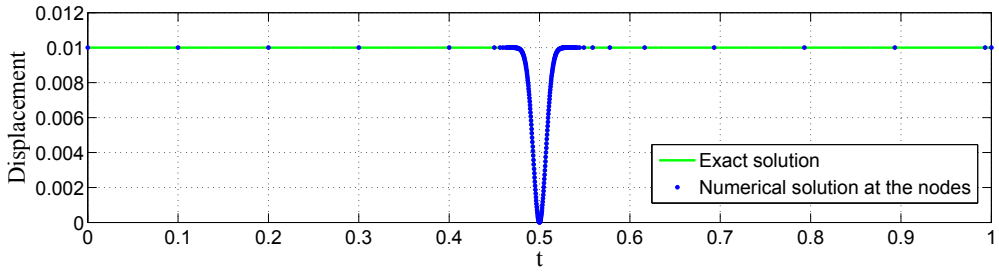


(b) Error

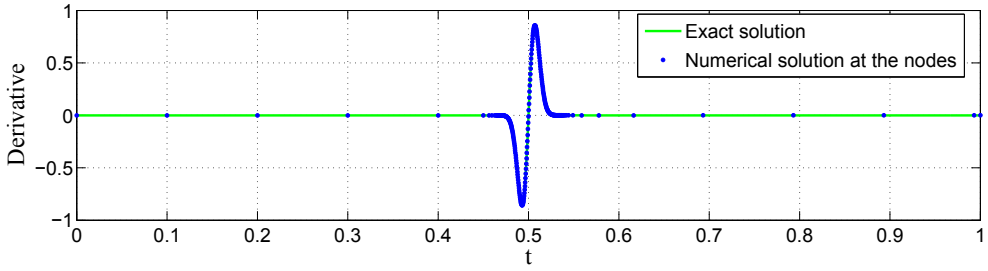
Figure 5: Example 5.2. The time step size trajectory and the error trajectory of $\|(\mathbf{u}-\mathbf{U})'\|_{\mathbf{M}}$ with $\epsilon = 1\mathrm{e}-1$, $k_{\min} = 3\mathrm{e}-4$.

We set $k_{\max} = 1$ and $\delta = 1/32$ in the computation (cf. Algorithm 4.2). Fig. 5 shows the error trajectory of $\|(\mathbf{u}-\mathbf{U})'\|_{\mathbf{M}}$ and the time step size trajectory, and the numerical solutions for $\mathbf{u}$ and $\mathbf{u}'$ are depicted in Fig. 6. Table 2 reports the numerical results when the adaptive algorithm was run for different values of ϵ and $k_{\min}$, where $N_* - 1$ is the total number of time iteration steps in the adaptive computation. (We adopted a uniform partition with the same iteration number $N_* - 1$ to carry out the computation.) The numerical results are shown in Table 3, where we see that Algorithm 4.2 is very efficient.

https://doi.org/10.4208/eajam.240715.050216a Published online by Cambridge University Press



(a) Numerical solution vs. exact solution for displacement



(b) Numerical solution vs. exact solution for derivative of displacement

Figure 6: Example 5.2. Curves of solutions and their derivatives on the first vehicle (Fig. 2) with $\epsilon = 1e-1$, $k_{\min} = 3e-4$.

Table 2: Example 5.2. Adaptive numerical results with different ϵ and $k_{\min}$.

ϵ	$k_{\min}$	η	$\|(\mathbf{u}-\mathbf{U})'\|_{L^\infty_{\mathbf{M}}(0,T)}$	N	N_*
1e-1	3e-4	1.0328e-1	3.7022e-2	263	275
1e-1	2e-4	4.5950e-2	1.6458e-2	375	385
2e-2	1e-4	1.1450e-2	4.1145e-3	739	751
2e-2	3e-5	1.1369e-3	4.0237e-4	2076	2092
5e-3	2e-5	4.9108e-4	1.7884e-4	3244	3261
5e-3	1e-5	2.8046e-4	1.7883e-4	5571	5592

Table 3: Example 5.2. Numerical results with uniform partitions.

N_*	η	$\|(\mathbf{u}-\mathbf{U})'\|_{L^\infty_{\mathbf{M}}(0,T)}$
275	1.5867e+1	4.7153
385	7.9931	2.7382
751	2.0694	7.2680e-1
2092	2.6252e-1	9.3779e-2
3261	1.0768e-1	3.8684e-2
5592	3.6518e-2	1.3157e-2

5.3. A practical application

Example 5.3 (The Pratt truss)**.** We also considered the vibration of a Pratt truss, which is a typical benchmark in structural analysis. The cross sectional area, nodes, elements and

https://doi.org/10.4208/eajam.240715.050216a Published online by Cambridge University Press

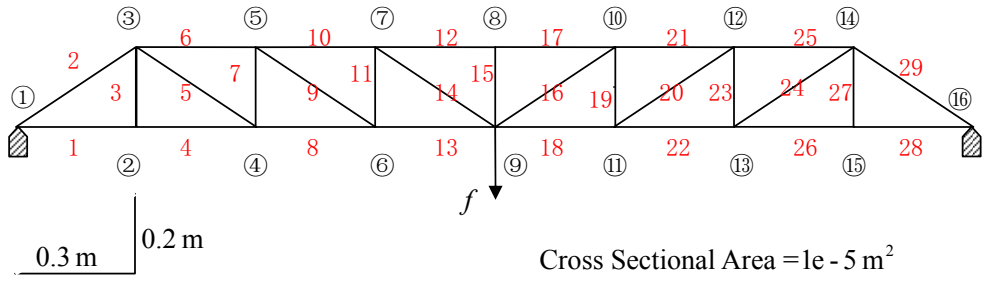


Figure 7: Example 5.3. The Pratt truss model.

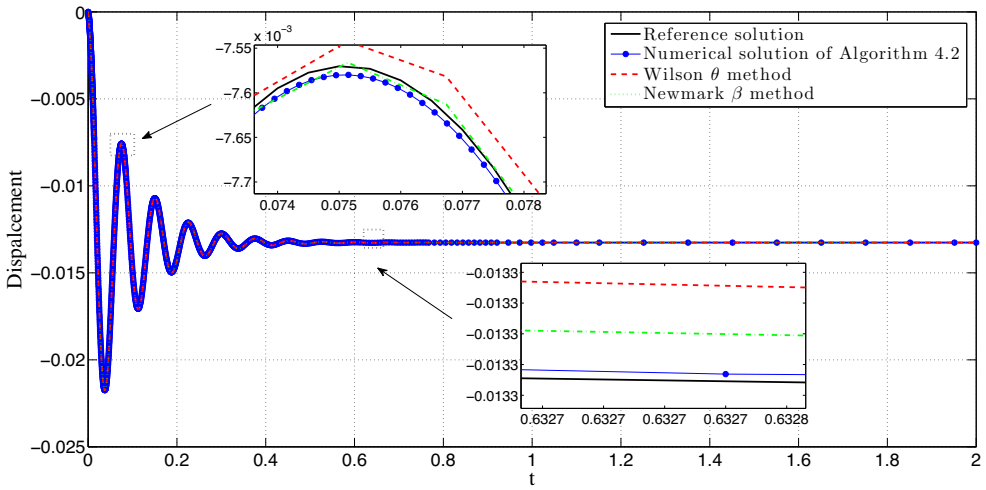


Figure 8: Example 5.3. Numerical solutions with different methods at Point 9.

length are shown in Fig. 7; and we took Young's modulus E to be 10^9 Pa, and the density $\rho = 2700$ kg/m^3. The Rayleigh damping coefficients adopted were $\alpha = 2 \times 10^{-2}$ and $\beta = 3 \times 10^{-3}$. The constant y-direction point force $f \equiv -10$ N only acts at the point 9 (the other points are force free). We assumed zero initial conditions, and used space bar elements — i.e. conforming P_1 elements in the axial direction.

We set $T = 2$ s, $k_{\max} = 1 \times 10^{-1}$, $k_{\min} = 5 \times 10^{-5}$, $\epsilon = 2 \times 10^{-2}$ and $\delta = 1/32$ in the computation — cf. Algorithm 4.2. Since this complex structure problem does not have a closed form solution, we computed a reference solution with a sufficiently small uniform time step size. Numerical results from Algorithm 4.2, the Wilson θ method corresponding to the parameter $\theta_0 = 1.4$ and the Newmark β method corresponding to the parameters $\alpha_0 = 0.25$ and $\beta_0 = 0.5$ are shown in Fig. 8 for comparison, where a uniform time step size $k = 1/N^*$ was used. In Fig. 10 we show the scaling deformation and the exact deformation effect at time $T = 0.05$ s. It is evident that Algorithm 4.2 is quite efficient for the Pratt truss problem.

https://doi.org/10.4208/eajam.240715.050216a Published online by Cambridge University Press

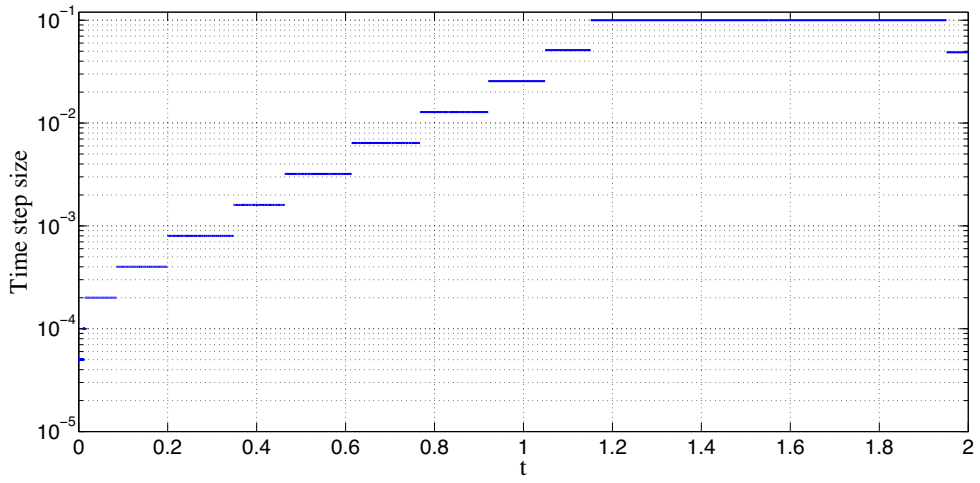


Figure 9: Example 5.3. The time step size trajectory.

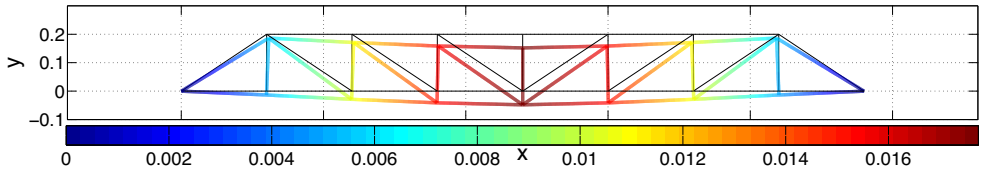


Figure 10: Example 5.3. The scaling deformation of the Pratt truss at $T = 0.05$ s.

6. Conclusion

Adaptive time stepping methods are very useful to numerically solve for the long-term evolution of a finite or infinite dimensional dynamical system, in various engineering and other applications. This work focused on designing and analysing adaptive time stepping methods for transient dynamic response analysis, frequently encountered in civil engineering for example. Using the energy method, we obtained optimal order *a posteriori* error estimates, which combined with an error equidistribution strategy and some ideas implicit in the Runge-Kutta-Felberg method led to an highly efficient adaptive time stepping method for transient dynamic response analysis.

In summary, our main observations from the numerical results reported in the last section are as follows.

- The *a posteriori* error estimators developed in this paper are reliable and efficient. The numerical results given in Example 5.1 showed that the *a posteriori* error estimators obtained are third-order accurate for the displacement and second-order accurate for the velocity, and coincide with the theoretical estimates given in Theorem 3.2.
- The adaptive time stepping method (Algorithm 4.2) is very efficient for solving the evolution problems under consideration, as we showed by comparing the numerical errors in using the uniform partition and adaptive partition — cf. Tables 2 and 3 in

https://doi.org/10.4208/eajam.240715.050216a Published online by Cambridge University Press

Example 5.2, and Fig. 8 in the application Example 5.3.

- The choice of the parameters $k_{\min}$, δ and ϵ affects the computational efficiency of the adaptive time stepping method (Algorithm 4.2). In particular, the choice of the lower bound of the time step size $k_{\min}$ is very critical. If it is too large, the total error may not be dominated by the prescribed error tolerance, and if too small the algorithm may lead to over-refinement. Although $k_{\min}$ can be chosen quite readily from numerical experience as shown in Table 2, in our ongoing work we intend to develop some other algorithms based on the adaptive algorithm developed in this paper, to tackle this issue.

Acknowledgments

The authors thank the referees for their valuable comments leading to great improvement of an earlier version of this article. The work was partly supported by NSFC (Grant Nos. 11171219 and 11571237) and the E-Institutes of Shanghai Municipal Education Commission (E03004).

References

[1] G. Akrivis and P. Chatzipantelidis, *A posteriori error estimates for the two-step backward differentiation formula method for parabolic equations*, SIAM J. Num. Anal. **48**, 109-132 (2010).
[2] G. Akrivis, C. Makridakis and R.H. Nochetto, *Galerkin and Runge-Kutta methods: Unified formulation, a posteriori error estimates and nodal superconvergence*, Num. Math. **118**, 429-456 (2011).
[3] G. Aksu and R. Ali, *Free vibration analysis of stiffened plates using finite difference method*, J. Sound Vib. **48**, 15-25 (1976).
[4] V. Arora, *Direct structural damping identification method using complex FRFs*, J. Sound Vib. **339**, 304-323 (2015).
[5] T. Caughey and M. Okelly, *Classical normal modes in damped linear dynamic systems*, J. Appl. Mech. **32**, 583-588 (1965).
[6] Z. Chen and J. Feng, *An adaptive finite element algorithm with reliable and efficient error control for linear parabolic problems*, Math. Comp. **73**, 1167-1193 (2004).
[7] R.W. Clough and J. Penzien, *Dynamics of Structures*, Third Edition, Computers & Structures, Inc. (2003).
[8] D. Cronin, *Eigenvalue and eigenvector determination for nonclassically damped dynamic systems*, Comp. Struct. **36**, 133-138 (1990).
[9] C. Farhat and E. Wilson, *Modal superposition dynamic analysis on concurrent multiprocessors*, Eng. Comp. **3**, 305-311 (1986).
[10] X. Feng, T. Tang and J. Yang, *Long time numerical simulations for phase-field problems using p-adaptive spectral deferred correction methods*, SIAM J. Sci. Comp. **37**, A271-A294 (2015).
[11] D.A. French, *A space-time finite element method for the wave equation*, Comp. Meth. Appl. Mech. Eng. **107**, 145-157 (1993).
[12] P. Heyliger and J. Reddy, *A higher order beam finite element for bending and vibration problems*, J. Sound Vib. **126**, 309-326 (1988).
[13] J. Huang, J. Lai and T. Tang, *An adaptive time stepping method with efficient error control for second-order evolution problems*, Sci. China Math. **56**, 2753-2771 (2013).

https://doi.org/10.4208/eajam.240715.050216a Published online by Cambridge University Press

[14] T.J. Hughes, *The Finite Element Method: Linear Static and Dynamic Finite Element Analysis*, Dover (2012).
[15] T.J. Hughes and G.M. Hulbert, *Space-time finite element methods for elastodynamics: Formulations and error estimates*, Comp. Meth. Appl. Mech. Eng. **66**, 339-363 (1988).
[16] G.M. Hulbert, T.J. Hughes, *Space-time finite element methods for second-order hyperbolic equations*, Comp. Meth. Appl. Mech. Eng. **84**, 327-348 (1990).
[17] T. Itoh, *Damped vibration mode superposition method for dynamic response analysis*, Earthquake Eng. Struct. Dyn. **2**, 47-57 (1973).
[18] C. Johnson, *Discontinuous Galerkin finite element methods for second order hyperbolic problems*, Comp. Meth. Appl. Mech. Eng. **107**, 117-129 (1993).
[19] D. Komatitsch, C. Barnes and J. Tromp, *Simulation of anisotropic wave propagation based upon a spectral element method*, Geophysics **65**, 1251-1260 (2000).
[20] M. Krawczuk, M. Palacz and W. Ostachowicz, *The dynamic analysis of a cracked Timoshenko beam by the spectral element method*, J. Sound Vib. **264**, 1139-1153 (2003).
[21] J. Lai and J. Huang, *An adaptive linear time stepping algorithm for second-order linear evolution problems*, Int. J. Num. Anal. Mod. **12**, 230-253 (2015).
[22] J. Lai, J. Huang and C. Chen, *Vibration analysis of plane elasticity problems by the c0-continuous time stepping finite element method*, Appl. Num. Math. **59**, 905-919 (2009).
[23] J. Lai, J. Huang and Z. Shi, *Vibration analysis for elastic multi-beam structures by the c0-continuous time-stepping finite element method*, Int. J. Num. Meth. Bio. **26**, 205-233 (2010).
[24] X.D. Li and N.-E. Wiberg, *Structural dynamic analysis by a time-discontinuous Galerkin finite element method*, Int. J. Num. Meth. Eng. **39**, 2131-2152 (1996).
[25] M. Liu and D. Gorman, *Formulation of Rayleigh damping and its extensions*, Comp. Struct. **57**, 277-285 (1995).
[26] R.H. Nochetto, G. Savaré and C. Verdi, *A posteriori error estimates for variable time-step discretizations of nonlinear evolution equations*, Commun. Pure Appl. Math. **53**, 525-589 (2000).
[27] K.S. Numayr, R.H. Haddad and M.A. Haddad, *Free vibration of composite plates using the finite difference method*, Thin-Walled Struct. **42**, 399-414 (2004).
[28] G.R. Olsen and G.N. Vanderplaats, *Method for nonlinear optimization with discrete design variables*, AIAA J. **27**, 1584-1589 (1989).
[29] Z. Qiao, Z. Zhang and T. Tang, *An adaptive time-stepping strategy for the molecular beam epitaxy models*, SIAM J. Sci. Comp. **33**, 1395-1414 (2011).
[30] D.A. Saravanos, P.R. Heyliger and D.A. Hopkins, *Layerwise mechanics and finite element for the dynamic analysis of piezoelectric composite plates*, Int. J. Solids Struct. **34**, 359-378 (1997).
[31] J. Stoer and R. Bulirsch, *Introduction to Numerical Analysis*, Vol. 12, Springer Science & Business Media (2002).
[32] Z. Zhang and Z. Qiao, *An adaptive time-stepping strategy for the Cahn-Hilliard equation*, Commun. Comp. Phys. **11**, 1261-1278 (2012).
[33] Z. Zhang, Y. Ma and Z. Qiao, *An adaptive time-stepping strategy for solving the phase field crystal model*, J. Comp. Phys. **249**, 204-215 (2013).

https://doi.org/10.4208/eajam.240715.050216a Published online by Cambridge University Press